JOURNAL OF GEOPHYSICAL RESEARCH, VOL. 107, NO. D21, 4589, doi:10.1029/2001JD001307, 2002

Retrieval of tropospheric ozone from simulations of limb spectral radiances as observed from space

S. A. Clough, J. R. Worden,[1] P. D. Brown,[2] and M. W. Shephard
Atmospheric and Environmental Research, Inc., Lexington, Massachusetts, USA

C. P. Rinsland
Atmospheric Sciences Division, NASA Langley Research Center, Hampton, Virginia, USA

R. Beer
Jet Propulsion Laboratory, Pasadena, California, USA

Received 19 September 2001; revised 24 January 2002; accepted 25 January 2002; published 12 November 2002.

[1] The frequent and direct remote sensing of the tropospheric ozone profile is a critical environmental measurement to be performed on a global scale by future satellite instruments. An approach has been developed for the retrieval of tropospheric ozone profiles from 9.6 μm limb-viewing clear-sky radiances generated for the spectral resolution and signal-to-noise of the Tropospheric Emission Spectrometer (TES). TES is a high-resolution Fourier transform spectrometer under development for NASA's Earth Observing System Aura platform (http://eos-chem.gsfc.nasa.gov/). The simulated radiance spectra are calculated from northern hemisphere midlatitude lidar profile measurements. The ozone profile retrieval and the associated errors are obtained as a function of atmospheric pressure level using the method of nonlinear least squares with regularization. In order to accelerate convergence a two-stage strategy has been applied in which the full profile retrieval has been preceded by a shape retrieval involving a smaller set of near independent parameters. Our analysis indicates that the O_3 profile can be retrieved from the TES limb measurements with a relative uncertainty of 5% (1σ) in the middle and upper troposphere. *INDEX TERMS:* 1640 Global Change: Remote sensing; 0322 Atmospheric Composition and Structure: Constituent sources and sinks; 0345 Atmospheric Composition and Structure: Pollution—urban and regional (0305); 0360 Atmospheric Composition and Structure: Transmission and scattering of radiation; 0365 Atmospheric Composition and Structure: Troposphere—composition and chemistry; *KEYWORDS:* remote sensing, ozone limb retrievals, tropospheric ozone, atmospheric constituents, Thermal Emission Spectrometer (TES)

Citation: Clough, S. A., J. R. Worden, P. D. Brown, M. W. Shephard, C. P. Rinsland, and R. Beer, Retrieval of tropospheric ozone from simulations of limb spectral radiances as observed from space, *J. Geophys. Res.*, *107*(D21), 4589, doi:10.1029/2001JD001307, 2002.

1. Introduction

[2] The frequent and direct global measurement of tropospheric ozone profiles represents an important measurement advance that will be first achieved by the Tropospheric Emission Spectrometer (TES). The TES instrument is a high spectral resolution Fourier transform spectrometer scheduled for flight onboard the Earth Observing System Aura platform. The TES instrument will record broadband limb and nadir emission spectra (650–3050 cm^{-1}) which will be analyzed to obtain global maps of the tropospheric profiles of O_3, H_2O, CO, NO, NO_2, CH_4, and HNO_3 [*Beer et al.*, 2001; *Beer and Glavich*, 1989]. In the past, satellite-based tropospheric O_3 measurements have been limited to seasonal average tropospheric total columns calculated by subtracting stratospheric columns from total column measurements [*Fishman et al.*, 1990; *Fishman*, 2000]. Previously, *Clough et al.* [1995] reported on a retrieval analysis based on simulated nadir spectral radiances calculated for the specifications of the TES instrument. Ozone profile retrieval errors of approximately ±5% (1σ) for a vertical resolution of 5 km in the middle and upper troposphere were estimated for background O_3 levels. The purpose of this paper is to quantify the TES tropospheric ozone limb retrieval capability as a function of pressure for cloud-free and aerosol-free conditions. Limb measurements have the advantage of higher vertical resolution and sensitivity relative to nadir observations. Our analysis is based on simulated limb radiance observations of the central region of the 9.6 μm ozone band at the TES operational resolution

[1]Now at Jet Propulsion Laboratory, Pasadena, California, USA.
[2]Now at Computer Sciences Corporation, Hartford, Connecticut, USA.

0148-0227/02/2001JD001307$09.00

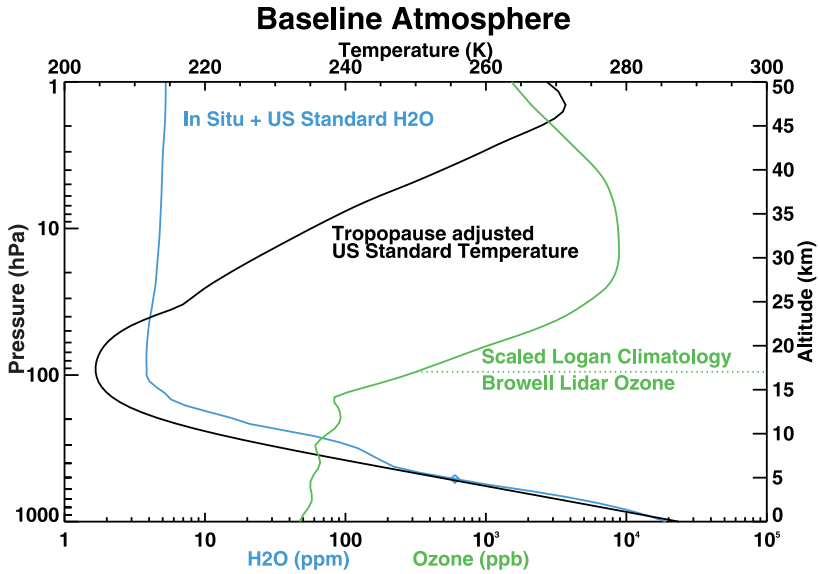

Figure 1. Profiles of temperature and water vapor used for the analysis. The ozone profile (green) is that used for the simulated radiances.

of 0.008 cm^{-1} (half width at half maximum (HWHM), unapodized).

2. Approach

[3] Operational limb measurements by TES will span latitudes of ±82° providing near global coverage under cloud-free conditions from near the surface to an altitude of 34 km using a 16-pixel detector linear array. The O_3 mixing ratio for a TES measurement can vary by three orders of magnitude, ranging from <10 ppbv in clean air near the surface to mixing ratios of 10000 ppbv at the midstratosphere O_3 peak. Our approach in this paper has been to select a high-quality midlatitude aircraft measurement sampling continental outflow in the western Pacific for simulation of a scientifically important example of a future midlatitude TES observation. Synthetic limb spectra for the TES spectral resolution of its 16 simultaneous limb measurements were generated from field measurements of O_3 and H_2O in combination with a climatological temperature profile. Retrieval of the O_3 profile was then performed from the simulated limb emission spectra with random noise added at the level expected for TES limb measurements near 10 μm. The results are then analyzed to quantify the expected TES O_3 retrieval capability under these conditions. The specification of the H_2O profile from correlative measurements is important because of the limitation the H_2O continuum imposes on sampling of the lower troposphere for a limb path. In fact, the H_2O continuum precludes the measurement of O_3 below 700 hPa in moist atmospheres.

2.1. Simulated Observation

[4] This study is based on a radiance simulation of the O_3, H_2O, and temperature profiles presented in Figure 1. The profiles of O_3 and H_2O are from observations off the coast of northern Japan during the PEM-West A campaign, flight 7. The O_3 profile was recorded with the Global Tropospheric Experiment (GTE) airborne Differential Absorption Lidar (DIAL) system on 24 September 1991 at 38°N latitude, 14°E longitude [*Browell et al.*, 1996]. The DIAL O_3 profile was extended from 17 km to the top of the atmosphere (100 km) by smoothly joining it to a climatological profile for the same latitude (J. Logan, private communication, 1999). The mixing ratio of H_2O below 10 km is based on in situ measurements obtained near the same latitude during the PEM-West A campaign. The temperature profile is based on the 1976 U.S. Standard Atmosphere. Profiles of other molecules for the forward model radiance simulation were adopted from standard reference profiles [*Anderson et al.*, 1986]. The combined profile set defines the atmosphere used in our analysis, both for forward model simulation and the retrieval analysis. The simulated spectral radiances are obtained with this atmosphere as illustrated in Figure 1, using the Line By Line Radiative Transfer Model (LBLRTM) [*Clough et al.*, 1995] with the HITRAN 1996 line parameters [*Rothman et al.*, 1998]. A TES nominal noise value of 2.58×10^{-8} W/(cm^2 sr cm^{-1}) appropriate to the source radiance has been added to the simulated spectral radiances.

2.2. Forward and Inverse Models

[5] Algorithms for both the forward atmospheric modeling and for the inverse procedure are essentially the same as those described by *Clough et al.* [1995]. Inversions from TES limb radiances are based on the Levenberg-Marquardt nonlinear least squares spectral fitting technique [*Levenberg*, 1944; *Marquardt*, 1963]. The method requires spectral radiances obtained from the forward radiative model and the Jacobians of the radiances with respect to changes in the O_3 profile. The Jacobians have been calculated with forward finite differences.

[6] For the present study the effects of systematic errors are not considered. The temperature profile, the H_2O profile, and the radiative effects of other interfering species are taken as known. The atmosphere is assumed to be aerosol free. We focus here on the retrieval of O_3 and the evaluation of the error in the profile due to instrumental

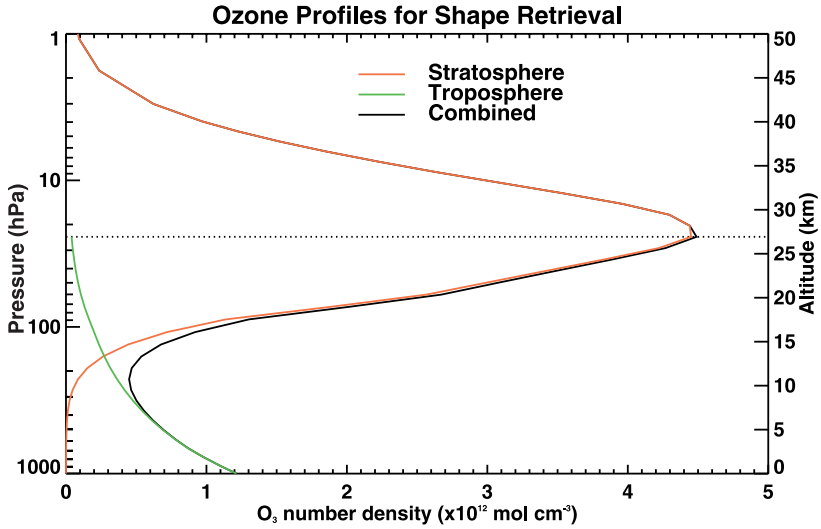

Figure 2. Stratospheric (red), tropospheric (green) and combined (black) profiles used for the robust shape retrieval.

noise only. Retrievals are based on fits to the 1027–1053 cm^{-1} region.

2.3. Retrieval Strategy

[7] Analogous with our strategy for the nadir case, a robust update of the initial guess profile using a reduced set of retrieval parameters and associated profile functions is performed. This is then followed by a global fit analysis on levels [e.g., *Carlotti et al.*, 2001]. It should be noted that for TES, 16 spectra associated with the 16-element detector array and corresponding to 16 tangent heights are measured simultaneously from the satellite. The objective of all procedures in the retrieval process is to minimize the variance of the spectral residuals. This update procedure provides accelerated convergence to the local minimum associated with the initial guess in the space of the reduced parameter set. In the nadir analysis the update of the initial guess profile was accomplished by performing a retrieval with two parameters: a scale factor for the stratospheric profile and a scale factor for the tropospheric profile. In this work, as a consequence of the higher vertical resolution of the limb observations, a more sophisticated approach is required. In our current approach, the ozone profile is decomposed into two profile components: one dominant in the stratosphere and the other in the troposphere. A modified version of the U.S. Standard ozone profile [*Anderson et al.*, 1986] has been adopted for the stratospheric component as indicated by the red curve in Figure 2 providing the number density as a function of log pressure. Four of the six parameters are used to update the stratospheric initial guess component: (1) a multiplicative scale factor for the stratospheric component; (2) a vertical displacement in log pressure; (3) a linear variation of the number density extending from the peak (dotted line in Figure 2) to lower values of log pressure; and (4) a linear variation of the number density extending from the peak to the surface.

[8] The tropospheric initial guess component has been taken as a constant 50 ppb. Two parameters are used for the initial guess update of the tropospheric component of the ozone volume mixing ratio (VMR): (1) a multiplicative scale factor applied to the constant VMR and (2) a change in the VMR lapse rate as a function of log pressure (taken as zero in the initial guess). The tropospheric component is defined as extending from the surface to 26 km at which point the discontinuity introduced by its termination is negligible. The full updated initial guess profile is obtained as the superposition of the two components and is effectively continuous from the surface to the top of the atmosphere. In Figure 2 the tropospheric and combined profiles are indicated in green and black, respectively.

[9] This approach for the robust initial guess update, we call the shape retrieval. The procedure provides a smooth representation of the true profile without introducing large representation errors associated with retrievals for a reduced set of levels (coarse vertical grid). The smoothing characteristics of the shape retrieval have not been analyzed in detail, since the resulting profile is only used as an improved guess for the subsequent global fit retrieval. The vertical grid for the global fit retrieval has been chosen to be consistent with UARS (Upper Atmosphere Research Satellite) grid, $P_I = 10^{(3\text{-}i/6)}$ with P_i in hPa and $I = 0,\ldots,N$. For the present limb application, regularization only comes into play in the global fit retrieval for the elements in the retrieval vector for which there is no ozone information: near the surface due to the atmospheric opacity associated with the water vapor continuum and in the high-altitude regime for which the ozone absorption is small. The entire spectrum is used in this analysis so that there is line of sight information being used in the altitude regime above the highest tangent altitude.

2.4. Forward Model

[10] The forward model provides the accelerated computation of simulated monochromatic radiances based on absorption and emission processes associated with each molecular species including the self-and air-broadened water vapor continuum [*Clough et al.*, 1989]. Model monochromatic radiances are calculated with a 45-level atmosphere extending from 0.09 to 100 km with a spacing of ~1.5 km to 40 km, with the level pressures consistent with a

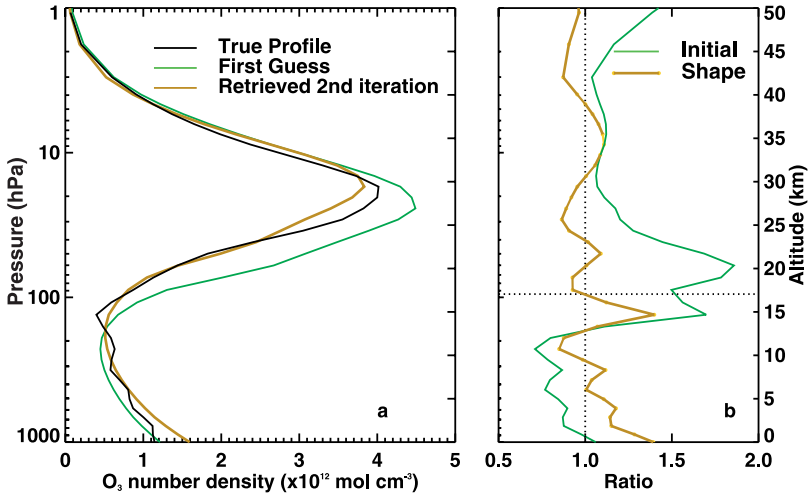

Figure 3. (a) The first guess profile (green), retrieved shape profile (yellow) and true profile (black). (b) Ratio of the first guess profile (green) and retrieved shape profile (yellow) to the true ozone profile.

superset of the UARS grid. Although log pressure has been used in the calculations throughout, altitude is used to facilitate the discussion. A Voigt line shape is used to calculate absorption coefficients with an algorithm based on linear interpolation between pre-calculated Voigt functions. Line coupling and the non-Lorentzian behavior of the wings of CO_2 lines are explicitly included. Spectroscopic line parameters and absorption cross-sections for both the forward model simulations and retrievals were taken from the 1996 HITRAN compilation [*Rothman et al.*, 1998]. The radiance associated with a given ray path includes the convolution of the monochromatic spectrum with the TES instrument spectral response function (0.008 cm^{-1} HWHM unapodized for the limb mode).

[11] The projection of the 16-element linear array at the limb is such that each pixel subtends 2.3 km (HWHM) in the vertical as viewed from the 705 km altitude of the satellite. The vertical radiance field at the satellite is obtained by calculating a series of rays from tangent levels from the surface to 40 km at 1.5 km spacing with refractive ray tracing [*Gallery et al.*, 1983]. The resulting angular radiance field at the satellite is then convolved with instrumental field of view (FOV) function associated with each of the 16 detectors. The interpolation for the radiance field between layers is a based on a quartic polynomial with continuous derivatives at the two interior points. Operationally, the pointing geometry will be established by the simultaneous retrieval of the array pointing angle and the temperature profile using CO_2 lines in the 700–800 cm^{-1} spectral region with the CO_2 profile assumed to be known.

3. Results and Discussion

[12] The results of the initial update retrieval (shape retrieval) are shown in Figure 3a. The profile used for the simulated radiances (Figure 1) is shown in black and is designated as the true profile. The initial guess shape profile is indicated in red and the retrieved shape profile using the six shape parameters is shown in yellow. All of the profiles have been mapped to the forward model grid. The retrieved profile is substantially closer to the true profile in all altitude regimes, but particularly in the critical regime of sharp

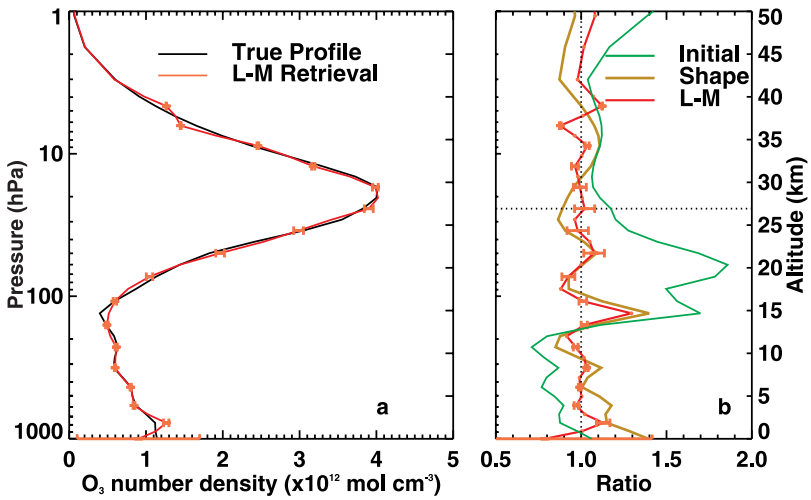

Figure 4. (a) The retrieved (red) and true (black) ozone profile. Errors are 1σ. (b) Ratio of the initial (green), retrieved shape (yellow) and retrieved level (red) results to the true ozone profile.

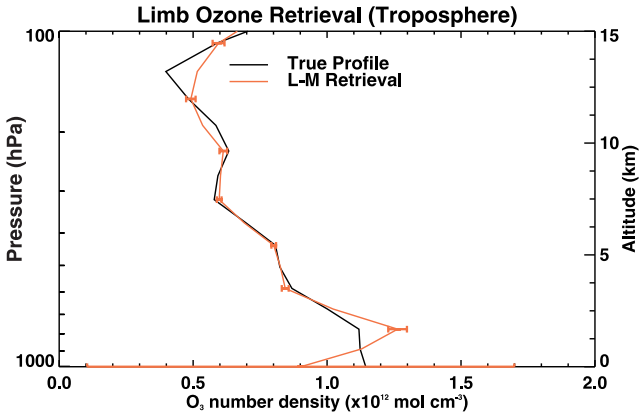

Figure 5. Plot of the retrieved (red) and true (black) ozone profiles for the troposphere. Errors are 1σ. The large error at the surface is due to water vapor continuum opacity.

ozone decrease in the lower stratosphere. This is seen more clearly in Figure 3b in which the ratios of the first guess and retrieved profile to the true profile are presented. The symbols on the retrieved profile ratio indicate the forward model levels. The results of the shape retrieval are such that subsequent level retrievals will effectively be in the linear regime, that is, the change in radiance due to a change in level number density is well represented by the relevant Jacobian. The result of the shape retrieval now serves as the first guess for the global level retrieval.

[13] For the global fit retrieval, 17 parameters have been retrieved corresponding to a grid consistent with the vertical resolution of the TES instrument. The spacing of the retrieval grid is ~2.3 km up to 36 km with 16 retrieval parameters. The seventeenth parameter is a multiplicative scaling factor for the profile above 36 km. The 2.3 km spacing is consistent with the tangent height spacing associated with the detector array. The results of the level retrieval are provided in Figure 4a. The error bars are 1σ values based on measurement error only. The ratios of the initial guess, shape, and level profiles to the true profile are shown in Figure 4b. The dotted horizontal line represents the upper limit of the profile measured by the lidar. The deviation of the retrieved profile ratio in the stratosphere from unity has maximum values of the order of 0.1, somewhat larger than the error due to measurement noise only. The principal cause of these deviations can be ascribed to representation error in which the mapping rules from the retrieval grid to the forward model grid do not properly describe the profile. The apparent discontinuity at 36 km is a result of not having adequate vertical resolution to describe the profile above that altitude. However, the errors in the stratosphere are for the most part consistent with the predicted errors.

[14] Since a principal objective of TES is the retrieval of ozone in the troposphere, the true and retrieved profiles are shown on an expanded scale in Figure 5. The retrieved profile tracks the smoothed lidar measurement extremely well except in the regime near the surface and the value at 14 km. The increased errors at the top of the boundary layer and at the surface are a consequence of the attenuation of the radiation due to the self-broadened water vapor continuum. No a priori constraint has been invoked in this study so that the large deviation at the surface has not been constrained and the error bar reflects the fact that minimal information is contained in the spectrum. The issue at 14 km is again one of representation error. The vertical resolution of the retrieval is not adequate to capture the ozone minimum at 14 km. There is a strong indication that it will be possible to retrieve information on a vertical grid finer than the HWHM of the TES FOV without a strong reliance on a priori information. This is currently under study.

[15] **Acknowledgments.** We would like to acknowledge an anonymous reviewer whose suggestions have contributed to an improved paper. Research at AER was supported through Science Team funding from JPL. Research at NASA Langley Research Center was supported by NASA through TES Science Team funding and the Atmospheric Chemistry and Modeling Program (ACMAP).

References

Anderson, G. P., S. A. Clough, F. X. Kneizys, J. W. Chetwynd, and E. P. Shettle, AFGL atmospheric constituent profiles (0–120 km), *Tech. Rep. AFGL-TR-86-0110*, Phillips Lab., Hanscom Air Force Base, Mass., 1986.

Beer, R., and T. A. Glavich, Remote sensing of the troposphere by infrared emission spectroscopy, *Proc. SPIE Int. Soc. Opt. Eng.*, *1129*, 42–48, 1989.

Beer, R., T. A. Glavich, and D. M. Rider, Tropospheric Emission spectrometer for the Earth Observing System's aura satellite, *Appl. Opt.*, *40*, 2356–2367, 2001.

Browell, E. V., et al., Large-scale air mass characteristics observed over the western Pacific during summertime, *J. Geophys. Res.*, *101*, 24,043–24,068, 1996.

Carlotti, M., B. M. Dinelli, P. Raspollini, and M. Ridolfi, Geo-fit approach to the analysis of limb-scanning satellite measurements, *Appl. Opt.*, *40*, 1872–1885, 2001.

Clough, S. A., F. X. Kneizys, and R. W. Davies, Line shape and the water vapor continuum, *Atmos. Res.*, *23*, 229–241, 1989.

Clough, S. A., C. P. Rinsland, and P. D. Brown, Retrieval of tropospheric ozone from simulations of nadir spectral radiances as observed from space, *J. Geophys. Res.*, *100*, 16,579–16,593, 1995.

Fishman, J., Observing tropospheric ozone from space, *Prog. Environ. Sci.*, *2*, 275–290, 2000.

Fishman, J., C. E. Watson, J. C. Larsen, and J. A. Logan, Distribution of tropospheric ozone determined from satellite data, *J. Geophys. Res.*, *95*, 3599–3617, 1990.

Gallery, W. O., F. X. Kneizys, and S. A. Clough, Air mass computer program for atmospheric transmittance/radiance calculation: FSCATM, *AFGL-TR-0065*, *Environ. Res. Pap.*, *828*, Air Force Geophys. Lab., Bedford, Mass., 1983.

Levenberg, K., A method for the solution of certain problems in least squares, *Q. Appl. Math.*, *2*, 164–168, 1944.

Marquardt, D., An algorithm for least squares estimation of nonlinear parameters, *SIAM J. Appl. Math.*, *11*, 431–441, 1963.

Rothman, L. R., et al., The HITRAN molecular spectroscopic database and HAWKS (HITRAN atmospheric workstation): 1996 edition, *J. Quant. Spectrosc. Radiat. Transfer*, *60*, 665–710, 1998.

R. Beer, Jet Propulsion Laboratory, 4800 Oak Grove Drive, MS 183-301, Pasadena, CA 91109, USA. (reinhard.beer@jpl.nasa.gov)

P. D. Brown, c/o Atmospheric and Environmental Research, Inc., 131 Hartwell Ave., Lexington, MA 02421-3126, USA. (pbrown@sherwoodlane.com)

S. A. Clough and M. W. Shephard, Atmospheric and Environmental Research, Inc., 131 Hartwell Avenue, Lexington, MA 02421-3126, USA. (sclough@aer.com; mshepar@aer.com)

C. P. Rinsland, Atmospheric Sciences Division, NASA Langley Research Center, Mail Stop 401A, Hampton, VA 23681, USA. (rinsland@mipsbox.larc.nasa.gov)

J. R. Worden, Jet Propulsion Laboratory, 4800 Oak Grove Drive, MS 183-301, Pasadena, CA 91109, USA. (jworden@jpl.nasa.gov)